CORE
Metadata, citation and similar papers at core.ac.uk
Provided by NASA Technical Reports Server

N O T I C E

THIS DOCUMENT HAS BEEN REPRODUCED FROM MICROFICHE. ALTHOUGH IT IS RECOGNIZED THAT CERTAIN PORTIONS ARE ILLEGIBLE, IT IS BEING RELEASED IN THE INTEREST OF MAKING AVAILABLE AS MUCH INFORMATION AS POSSIBLE

DR-A

UNIVERSITY OF HAWAII

INSTITUTE FOR ASTRONOMY

(NASA-CR-164231) INFRARED AND RADIO OBSERVATIONS OF W51: ANOTHER ORION-KL AT A DISTANCE OF 7kPC (Hawaii Univ.) 28 p HC A03/MF A01 CSCL 03A

N81-25005

Unclas G3/89 15026

RECEIVED NASA STI FACILITY ACCESS DEPT.

UNIVERSITY·OF·HAWAII
UA·MAU·KE·EA·O·KA·AINA·I·KA·PONO
1907

AP. J.
MAN. 3159

INFRARED AND RADIO OBSERVATIONS OF W51: ANOTHER ORION-KL AT A DISTANCE OF 7 kpc?

R. Genzel[1]*, E.E. Becklin[2], C.G. Wynn-Williams[2],*
J.M. Moran[3], M.J. Reid[3], D.T. Jaffe[3],
D. Downes[4]

Received _____

[1]Harvard-Smithsonian Center for Astrophysics, Cambridge, Mass., and Dept. of Physics, University of California, Berkeley.

[2]Institute for Astronomy, University of Hawaii.

[3]Harvard-Smithsonian Center for Astrophysics, Cambridge, Mass.

[4]Institut de Radio Astronomie Millimetrique, Grenoble, France.

*Visiting Astronomer, Infrared Telescope Facility which is operated by the University of Hawaii for the National Aeronautics and Space Administration.

ABSTRACT

We report high resolution infrared and radio continuum observations of the W51 region. The bright infrared source W51-IRS2 has at least three components with different physical and evolutionary properties. The spatial distribution and the near infrared spectra of the components in IRS2 are remarkably similar to, but more luminous than those found in Orion, where an HII region of comparable linear size is also located close to a cluster of compact infrared sources (the BN-KL complex). The characteristics of the nearby W51-NORTH H_2O maser source, and the detection of 2 μm H_2 quadrupole emission in IRS2 indicate that the mass loss phenomena found in Orion-KL also exist in W51.

In contrast to W51-NORTH, there is no compact 20 μm source associated with W51-MAIN, the second strong H_2O maser in this region. This result may be explicable in terms of differences in the gas and dust distribution around the sources.

The spatial distribution of 20 μm continuum radiation from the neighboring infrared source W51-IRS1 follows closely that of the radio continuum emission, and may be interpreted as arising from dust heated by Ly-α within the extended HII region.

Subject Headings: Infrared Sources

Infrared: Spectra - Masers

Nebulae: Individual - Radio

Sources: General

Stars: Formation

I. INTRODUCTION

W51 is a well-studied complex of radio continuum sources and giant molecular clouds at a distance of 7 kpc (e.g. Bieging 1975). The two strong radio H II regions W51-d and W51-e (Martin 1972; Scott 1978) are also bright sources in the 5-500 μm wavelength range (W51-IRS2 and W51-IRS1: Wynn-Williams, Becklin and Neugebauer 1974; Harvey, Hoffmann and Campbell 1975; Thronson and Harper 1979; Erickson and Tokunaga 1980; Hackwell, Grasdalen and Gehrz, 1981). Each of these sources is associated with an intense 22 GHz H_2O maser (W51-NORTH and W51-MAIN: Genzel and Downes 1977), the kinematics and the distances of which have been recently determined by the measurement of the proper motions of the brightest maser features (Genzel et al. 1981a; Schneps et al. 1981). In this paper, we report new high resolution radio continuum and infrared observations and discuss the spatial and energetic relationships among the infrared, radio continuum and maser sources.

II. OBSERVATIONS AND DATA REDUCTION

a) Infrared Observations

The infrared continuum observations were made at Mauna Kea, Hawaii, in May and July 1980 with a gallium-doped germanium bolometer mounted on the 3-m Infrared Telescope Facility (IRTF). We mapped the region containing W51-IRS1 and W51-IRS2 at 20 μm with a beam of 6" (FWHP) and a chopper throw of 2' in an East-West direction (Figure 1). In addition, the central region around IRS2 was mapped at high resolution (2") at 8 and 20 μm and a North-South chopper throw of 15" (Figure 2). Finally, we mapped the region around the strong H_2O source W51-MAIN (dotted rectangle in Figure 1) at 20 μm with a 2" aperture and 15"

North-South throw. In the 6" resolution maps, the grid spacing was 4", and in the 2" resolution maps, the grid spacing was 1". We checked the pointing every 5 to 15 minutes by peaking up on IRS2. The tracking stability of the telescope was significantly better than 1" over that time span; the source positions are therefore accurate to about 0.5" relative to the peak of IRS2. Angular offsets between observations using different filters were calibrated on β Peg, allowing us to determine relative positions at different wavelengths to an accuracy of better than 0.5". We determined the absolute position of the peak of IRS2 at 20 μm with a 2" aperture by offsetting from several nearby SAO stars and from two stars very close to the source whose positions were determined from Palomar Sky Survey plates. The resulting absolute position for IRS2 (Table 1) is accurate to ± 1". The 1 sigma noise level at 20 μm ($\Delta\lambda$ = 9 μm) was equivalent to about 1 Jy per beam area for the maps at 2" resolution and about 2 Jy per beam area for the 6" maps. At 7.9 μm ($\Delta\lambda$ = 0.7 μm) the noise was about 0.5 Jy per beam area. We also made photometric measurements at two positions in IRS2, with a 2" beam, at wavelengths between 2.2 and 20 μm; the filters were the same as those used by Downes et al. (1981) with the addition of a 10.3 μm filter with width 1.2 μm. The photometry was calibrated relative to β Peg and 4 Lac and is accurate to about 15%.

b) Radio Continuum Observations

The radio continuum observations at 5 and 15 GHz were made in December 1979 with the Very Large Array (VLA). We observed W51 over 7 hours, during which 10 minute observations on-source at 2 cm and 6 cm were interspersed with short calibrations on the sources 2005 + 403 and

2134 + 004. The absolute positions of these calibrators are known to better than ± 0.2"; we assumed flux densities at 5 and 15 GHz of 4 and 4 Jy for 2005 + 403 and 10.5 and 7 Jy for 2134 + 004. The flux density scale is accurate to ± 20% at 6 cm and ± 30% at 2 cm and the derived absolute positions are accurate to ± 0.2". The maps were made with the standard VLA reduction programs at the National Radio Astronomy Observatory*

---

*The National Radio Astronomy Observatory is operated by the Associated Universities, Inc., under contract with the National Science Foundation.

---

in Charlottesville, Virginia, and were CLEANED (Hogbom 1974) to improve the dynamic range. In a second step, we used the CLEAN components of the initial map in a self-calibration routine developed by Schwab (1980) to adjust optimally the amplitudes and phases. This method is especially useful at 15 GHz, where the telescope pointing is critical and phase variations due to atmospheric fluctuations are large.

III. Results

a) W51-IRS1

Figure 1 (left) shows the distribution of 20 μm emission in W51 at a resolution of 6". The brightness distribution of 20 μm continuum radiation from IRS1 is extended, complex, and clearly separated from the compact source IRS2. The 5 GHz map by Scott (1978) made with the Cambridge 5 km telescope has similar resolution to our infrared map, and is superimposed on the 20 μm contours in Figure 1 (right). The agreement between the morphologies of the 5 GHz free-free continuum emission and

the 20 μm radiation is excellent: the radio free-free and infrared distributions agree in the shape of the extended emission and in the positions and sizes of major components or ridges. However, as shown by Wynn-Williams et al., (1974), the infrared emission at 20 μm is nearly two orders of magnitude larger than that expected from free-free emission and probably comes from hot dust.

The agreement between the maps provides support for the view that most of the dust which radiates at 20 μm lies within the HII region and is heated by absorption of Lyman-α photons liberated by the recombinations in the ionized gas, as suggested by several authors (e.g., Wright 1973; Wynn-Williams and Becklin 1974). As pointed out by Harwit et al. (1972) the equilibrium temperature of dust grains heated in this way is only a very weak function of the local electron density in an HII region; if this variation is ignored then the ratio of infrared to radio volume emissivity will be uniform throughout the ionized region, and the close correspondence between the 6 cm and 20 μm maps is readily explained. If direct starlight from a star or stars close to the centroid of the HII region were the dominant energy source for the dust, the close agreement between infrared and radio emission would be largely fortuitous.

Quantitative support for the conclusion that the dust is heated predominantly by Ly-α radiation is obtained from the ratio of the surface brightness at 20 μm to that at 5 GHz. In Appendix A we calculcate what this ratio should be under the assumption that all of the Lyman-α energy absorbed by the grains is emitted at a single temperature T_g (see also Wynn-Williams et al. 1977). It is found that the ratio $S_{20\mu m}/S_{5GHz}$ lies

in the range 25-60 if the dust temperature is in the range 100-400 K, and the electron temperature is 10^4K. Loss of Lyman-α radiation by two-photon or other processes may reduce this theoretical ratio by up to about 30% (Mezger, Smith and Churchwell, 1974). From a comparison of the surface brightness of infrared and radio wavelengths we find that the ratio for $S_{20\mu m}/S_{5GHz}$ has the value 75 $\pm$ 30 over most of the face of HII region, a comparable range to that predicted in the assumption that Lyman-α is probably the predominant source of heating of the dust.

The observed energy distribution of W51-IRS1 more resembles a power law with slope -3.5 than a blackbody (Wynn-Williams et al. 1974), implying that dust is present with a wide variety of temperatures. The comparison of 20 μm with 5 GHz emission may therefore also be made by equating the infrared luminosity shortward of some wavelength λ_{max} with the Lyman-α heating. Using the formula in Appendix A, the predicted ratio of $S_{20\mu m}/S_{5GHz}$ is 98, on the assumption that $T_e = 10^4$K, $\beta = 3.5$, $f = 1$ and $\lambda_{max} = 25$ μm. This result implies that all the luminosity shortward of 25 μm can be supplied by Ly-α heating, as suggested by Wynn-Williams and Becklin (1974).

The spatial morphology of the radio and infrared emission indicates that W51-IRS1 is an extended HII region powered by a central cluster of early O stars. Molecular line data (Fomalont and Weliachew 1973), and continuum observations at 400 μm (Becklin, Telesco and Hildebrand 1981) suggest that the density of the molecular cloud increases eastward from IRS2 towards IRS1. These observations, and the sharp western ridge of the radio and infrared emission, may therefore indicate that the HII region lies at the edge of this dense molecular cloud; the south-eastern extension in the radio and infrared map suggests that the HII region may, in fact, partially surround the molecular cloud.

b) W51-IRS2

Figure 2 summarizes our infrared and radio observations of the region around the compact infrared source W51-IRS2. The bottom and middle parts of the Figure are the IRTF maps at 8 and 20 μm with a resolution of 2". The top part of Figure 2 shows the 2 cm VLA contours, the positions of the H_2O maser spots (Downes et al. 1979; Schneps et al. 1981), and the peaks of the 20 and 8 μm maps. In addition, the 20 and 40% contours of our 6 cm VLA map are shown dashed to emphasize the more extended radio emission.

The most important conclusion to be drawn from Figure 2 is that the infrared peaks at 8 and 20 μm do not coincide with the centroid of the compact radio H II region W51-d. However, the infrared maps show an elongation to the West which agrees quite well in position and size with the 2 cm radio contours. We identify this elongation of the infrared emission with the compact H II region and conclude that the more intense eastern peak of the infrared emission represents a second source of energy in IRS2. Spectrophotometric observations from 2.2 to 20 μm taken at the peak of the 20 μm emission and at position 4"W, 2.5" N of it support this picture (Figure 3) by demonstrating that the two regions have different energy distributions; the infrared source associated with the H II region shows a power-law spectrum with index -3.3 between 2 and 20 μm with no silicate feature at 9.7 μm, while the stronger, eastern source shows a more rounded blackbody spectrum with a deep silicate feature.

The 8 and 20 μm sizes of the western source are comparable, and the the ratio of 20 μm to radio brightness (Figure 2) is 100 ± 30. As discussed above for IRS1, these observed characteristics are as expected for hot dust within a compact H II region. We will henceforth call the infrared source associated with the H II region "IRS2(H II)," and,

the more intense source to the southeast "IRS2(H_2O)."

The stronger, eastern source IRS2(H_2O) appears to have at least two components of different color temperature, since the position of maximum emission changes with wavelength. The peak position of the "hot" component, which dominates between 2 μm and 8 μm, is 0.5" W and 0.8" S of the peak at 12.5 and 20 μm where the "cool" component is strongest. The 20 μm map also indicates that the cool component is extended over $\geq$ 3" (3 10^{17} cm), whereas the 8 μm source may only be slightly resolved in north-south direction. The hot component of IRS2(H_2O) is very close (1.6" $\pm$ 1.0") to the most intense center of H_2O maser activity, the "Dominant Center" (Downes et al. 1979). If the 8 and 20 μm maps of IRS2 are shifted to an optimal agreement with the radio continuum contours, the hot component is even closer (0.5" $\pm$ 0.5") to the H_2O peak. It is therefore likely that the H_2O maser source is associated with the "hot" component of IRS2(H_2O).

c) W51-MAIN and the Ultra-compact H II regions

The dotted rectangle in Figure 1 marks the region which contains the strong H_2O maser source W51-MAIN (the northernmost group of black dots), as well as two weaker "centers of H_2O activity," and two ground state OH maser sources at 1.7 GHz (Benson and Mutel, 1980) associated with two ultra-compact H II regions Scott (1978, see Table 1). Figure 1 (right) shows that there is weak extended emission of $\leq$ 15 Jy per 6" beam near the compact H II regions but no recognizable peak (see also Hackwell, Grasdalen and Gehrz 1981). We mapped the dotted region at 2" resolution and found a 3σ upper limit to any compact 20 μm source ($\leq$ 2") of 3 Jy.

IV. Discussion

a) W51-IRS2: Another Orion-KL

The low angular resolution of infrared and radio observations of distant star formation regions has in general permitted only simple geometric and energetic models. On the other hand, the few nearby regions of active star formation, in particular the Orion-KL region, show a wealth of complexity. Our observations of W51-IRS2 indicate that the characteristics of the Orion-KL region may be found in other regions of active star formation. The two sources are remarkably similar in the following way:

1) Morphology

In Orion-KL, a "compact" H II region of size $9\ 10^{17}$ cm(= 8", if Orion were at a distance of 7 kpc) is adjacent ($4\ 10^{17}$ cm = 4" at 7 kpc) to a cluster of 5-20 μm infrared sources (the BN-KL region; Rieke, Low and Kleinmann 1973; Wynn-Williams and Becklin 1974). The BN-KL complex dominates the 10-1000 μm appearance of the Orion region, and is generally thought to contain a cluster of young OB stars associated with the Orion Molecular Cloud and independent of the Trapezium stellar cluster which powers the radio HII region (e.g. Zuckerman 1973; Wynn-Williams and Becklin 1974). The infrared spectrum of the BN-KL region has a deep silicate absorption feature (Downes et al. 1981; Aitken et al. 1981), whereas the H II region shows a flat spectrum with silicate emission (Stein and Gillett, 1969). This separation into the Trapezium and the BN-KL regions is parallel to the separation into IRS2(H II) and IRS2(H_2O) in W51. Within the BN-KL region, size and peak position of the infrared emission change with wavelength: between 1 and 10 μm, two

compact, hot ($T_c \gtrsim$ 350 K) objects (BN and IRc2) dominate, whereas at wavelengths $\gtrsim$ 20 μm the most luminous source is the extended, cool ($T_c \sim$150 K) KL nebula which is about 12" south of BN (Downes et al 1981). The hot and cool components of IRS2(H_2O) may be the analogous features in W51. Finally, again in accord with W51, the strong H_2O maser source in Orion-KL is associated with one of the hot objects, IRc2 (Downes et al. 1981).

2) Kinematics

The measurement of proper motions of H_2O maser features in Orion-KL has shown that the maser cloudlets are expanding from a central point near IRc2 (Genzel et al. 1981b). The expansion seen directly by the transverse motions of the H_2O masers has also been deduced indirectly from the broad lineshapes of several "thermal" molecular lines indicating a general outflow of material with high mass loss rates (e.g. Zuckerman, Kuiper and Rodriquez-Kuiper 1976; Scoville 1980). The radial and proper motion data of H_2O masers in W51-NORTH and W51-MAIN also can be explained by the interaction of a strong stellar wind and with a surrounding dense molecular cloud (Schneps et al. 1981; Genzel et al. 1981a) and may indicate mass loss phenomena similar to those in Orion-KL. This inference is supported by the recent detection of 2 μm quadrupole line emission of molecular hydrogen in IRS2 by Beckwith and Zuckerman (1981). The integrated luminosities of typical H_2O maser lines (assuming isotropic emission) in

W51 are greater than those in Orion by factors of 20 to 50. However, the 2 μm H_2 lines in W51-IRS2 are much less luminous than those in Orion (Beckwith and Zuckerman 1981). This may indicate that the physical conditions in the outflow are different and/or that the linear size of the 2 μm H_2 source in W51 is smaller than that in Orion and/or that the 2 μm extinction in the two clouds is different. The linear size of the dominant H_2O center in W51-NORTH is $\sim 2\ 10^{16}$ cm, whereas the H_2O outflow in Orion has an extent of $> 3\ 10^{17}$ cm.

3) Luminosity

The chief difference between the two regions is that W51-IRS2 is considerably more luminous than Orion, when measurements at the same linear resolution are compared. The infrared bolometric luminosity of W51-IRS2 has been measured with 30" (1.2 pc) beam by Erickson and Tokunaga (1980) and Thronson and Harper (1979); the luminosity is about 3×10^6 $L_\odot$. At the distance of Orion 1.2 pc corresponds to a beam about 7' across; the luminosity of this region is of order 5×10^5 $L_\odot$ (Harper 1974). The bolometric luminosity of the whole W51-IRS2 region, including both the H II region and the molecular cloud sources, is therefore about six times higher than that of a region in Orion which encompasses both the molecular cloud sources and the H II region.

Because of the poor resolution in the infrared measurements at $\lambda > 20$ μm, it is not possible to measure independently the bolometric luminosities of IRS2(H II) and IRS2(H_2O). We can, however, compare the flux densities in the 20 μm band; the flux density of the KL region of Orion at 20 μm is about 10^4 Jy in a 30 arc sec (0.07 pc) beam (Sutton, Becklin and Neugebauer 1974). The same linear resolution in W51 corresponds to a 2.1 arc sec beam; our 2 arc sec measurements give a flux of 200 Jy

in a beam of this size. The 20 μm luminosity of W51-IRS2 is therefore a factor of about 4 times higher than that of the KL nebula at a linear resolution of 0.07 pc.

b) W51-MAIN: The Lack of 20μm Emission

W51-MAIN is one of the brightest maser sources in the sky; in the luminosity, kinematics and spatial distribution of its H_2O features, it strongly resembles W51-NORTH, the maser source associated with IRS2. Despite this similarity, we have not detected it at 20 μm. Extinction by a dense molecular cloud in front of W51-MAIN may explain this lack of infrared emission. Evidence for such an obscuring cloud is provided by the lack of 20 μm emission from the ultra-compact H II regions W51-e_1 and W51-e_2. If there is dust heated by Lyα within these H II regions, the radio flux densities of ∿0.15 Jy at 5 GHz (Scott 1978) imply 20 μm flux densities of 5 to 15 Jy, using the same arguments as we have for IRS1 and IRS 2 (H II) (see Section III.1 and Appendix A). Our 3σ upper limit of 3 Jy therefore imply that there is probably at least one magnitude of extinction at 20 μm. This extinction could be related to the molecular cloud whose presence to the east of IRS1 can be inferred from the 400 μm observations by Becklin, et al. (1981) and the morphology of IRS1 (Section IIIa). Finally, molecular line observations show that the optical depths of the H_2CO and NH_3 lines in the 58 km s^{-1} cloud also peak in the vicinity of W51-MAIN and the ultra-compact H II regions (Fomalont and Weliachew 1973; Matsakis et al. 1980). If there were an infrared source associated with W51-MAIN with a luminosity comparable to IRS2, the inferred extinction would have to be as high as 4.5 mag at 20 μm. Similar large extinctions have been estimated for other regions like K3-50 C1, and Sgr B2 (Wynn-Williams et al 1977; Gatley et al. 1978).

The only significant difference between the H_2O sources W51-MAIN and W51-NORTH may be the radial velocity distribution of the maser features. Almost all features in W51-MAIN are redshifted with respect to the rest velocity of the molecular cloud (e.g. Genzel et al. 1979), while most of the masers in W51-NORTH are blueshifted. It is possible that asymmetries in the distribution of matter around the maser sources may explain both the infrared and maser observations. A cloud of density $\gtrsim 10^6$ cm^{-3} and scale size $\gtrsim 10^{17}$ cm (like the core of OMC1) in front of W51-MAIN would have a large optical depth at 20 μm and could also effectively block the escape of blueshifted high velocity material (e.g. Genzel et al. 1979).

While the strong H_2O masers in Orion-KL and W51-IRS2 are associated with hot, compact sources of infrared emission, W51-MAIN and several other bright maser sources lack associated strong infrared emission shortward of 20 μm (e.g. Forster et al. 1978). All these maser sources, however, are similar to the maser in Orion-KL and W51-IRS2 and may indicate mass loss phenomena in regions of active star formation. We suggest that this lack of infrared emission might be caused by extinction from an inhomogeneous distribution of dense material surrounding the source of outflow. The amount of infrared emission associated with a maser source could be correlated with the radial velocity distribution of the outflow, if density inhomogeneities not only block the escape of infrared radiation, but also the escape of the outflow itself. Since asymmetries in the velocity profiles of maser emission have been noted for quite a number of H_2O sources with high velocity emission (Heckman and Sullivan 1976; Morris 1976; Goss et al. 1976; Genzel and Downes 1977; Rodriguez et al. 1980), an obvious test of this idea would be an infrared search toward

those masers with mainly blue-shifted high velocity features.

V. CONCLUSIONS

High resolution infrared and radio mapping of W51 have shown the following:

a) W51-IRS1 has a very similar appearance at 20 μm and 5 GHz; this agreement provides quantitative support for the view that most of the heating of the dust is by Lyman-α radiation.

b) At least three physically dissimilar infrared sources comprise W51-IRS2. In its size, morphology and kinematics W51-IRS2 resembles the Orion nebula and molecular cloud, but its luminosity is several times larger.

c) No infrared emission was detected from H_2O maser source W51-MAIN: in contrast, strong 20 μm emission is associated with the W51-NORTH maser. The difference in infrared properties may result from the presence of a thick obscuring cloud in front of W51-MAIN. This could may also influence the kinematics of H_2O outflow itself.

ACKNOWLEDGMENTS

We thank the IRTF staff, C. Kaminski, A.J.B. Downes and C. Fang for help with the infrared observations and data reduction. We are grateful to F. Schwab, and E. Fomalont for valuable advice and to A. P. Lane for assistance with the V.L.A. data reduction. B. Zuckerman, S. Beckwith, R. Hildebrand, C. Telesco and J. Benson provided data prior to publication. This research was supported by NASA contract NASW-3159 and NSF grant AST 78-26028.

APPENDIX A

RATIO OF INFRARED TO RADIO FLUX DENSITY FOR GRAIN HEATING BY Ly-α PHOTONS

The relationship between rate of production of ionizing photons, N_{Lyc}, and the free-free radio flux density S_{RAD} has been calculated by Rubin (1968). With slight changes of units his relationship is

$$N_{Lyc} = 7.54\times10^{46}\left(\frac{S_{RAD}}{Jy}\right)\left(\frac{D}{kpc}\right)^{2}\left(\frac{\nu}{GHz}\right)^{0.1}\left(\frac{T_e}{10^4 K}\right)^{-0.45} \text{ photons } s^{-1}. \quad (1)$$

where D is the distance to the H II region, T_e is its electron temperature and ν the radio observing frequency.

If a fraction f of the ionizations lead to the production of a Ly-α photon that is absorbed by dust grains (as opposed to, for example, a two-photon pair or a Ly-α photon which escapes the nebula) then the wavelength-integrated infrared flux S_{TOT} at the Earth is given by

$$S_{TOT} = \frac{f h\nu_{Ly\alpha} N_{Lyc}}{4\pi\,(3.086\times10^{19})^2}\left(\frac{D}{kpc}\right)^{-2} \quad Wm^{-2} \quad (2)$$

where $h\nu_{Ly\alpha}$ is the energy of a Lyman-α photon, namely 1.64×10^{-18} W. If the dust grains radiate as a grey-body at a temperature T_g then the infrared flux density S_{IR} at a wavelength λ is given by a a normalized form of the Planck law.

$$\frac{S_{IR}}{S_{tot}} = \frac{15 h^4 c^3}{\pi^4 k^4 \lambda^3 T_g^4} \left(e^{\frac{hc}{\lambda k T_g}} - 1 \right)^{-1} \quad Hz^{-1} \tag{3}$$

Combining equations 1-3 leads to an expression for the ratio of the infrared to radio flux density at a wavelength λ (in μm) at a temperature T_g (°K)

$$\frac{S_{IR}}{S_{RAD}} = \frac{2.28 \times 10^6 f}{\lambda^3 T_g^4} \left(\frac{\nu}{GHz} \right)^{0.1} \left(\frac{T_e}{10^4 K} \right)^{-0.45} \left(e^{\frac{14388}{\lambda T_g}} - 1 \right)^{-1} \tag{4}$$

An alternative way of comparing infrared and radio luminosities is to equate the Lyman-α heating with the luminosity emitted as a power law at infrared wavelengths shortward of some wavelength λ_{max}:

$$S_{IR} = const \times \lambda^{\beta} \tag{5}$$

In this case the ratio of the infrared to radio flux density is given by

$$\frac{S_{IR}}{S_{RAD}} = 3.43 f (\beta - 1) \lambda_{max} \left(\frac{\lambda}{\lambda_{max}} \right)^{\beta} \left(\frac{\nu}{GHz} \right)^{0.1} \left(\frac{T_e}{10^4 K} \right)^{-0.45} \tag{6}$$

TABLE 1 POSITIONS OF COMPACT SOURCES IN W51

Source	RA. (1950)	DEC. (1950)	Remarks
IRS2(HII)	$19^h\ 21^m\ 22^s.30 \pm 0^s.05$	14° 25' 14".8 ± 1".0	Average of 8 and 20 μm, 2" resolution
IRS2(H_2O) 8μm	$19^h\ 21^m\ 22^s.53 \pm 0^s.05$	14° 25' 12".9 ± 1".0	Peak of the 2" maps
IRS2(H_2O) 20μm	$19^h\ 21^m\ 22^s.56 \pm 0^s.05$	14° 25' 13".7 ± 1".0	
H II-d	$19^h\ 21^m\ 22^s.27 \pm 0^s.02$	14° 25' 15".0 ± 0".2	2 cm VLA peak
H II-e_1	$19^h\ 21^m\ 26^s.12 \pm 0^s.01$	14° 24' 32".6 ± 0".2	Scott 1978
H II-e_2	$19^h\ 21^m\ 26^s.22 \pm 0^s.01$	14° 24' 41".0 ± 0".2	
OH (1)	$19^h\ 21^m\ 26^s.22 \pm 0^s.03$	14° 24' 41".6 ± 1".0	Moran et al. 1981; Mader, Johnston & Moran 1978
OH (2)	$19^h\ 21^m\ 26^s.28 \pm 0^s.03$	14° 24' 36".1 ± 1".0	Benson, private communication.
H_2O-NORTH	$19^h\ 21^m\ 22^s.40 \pm 0^s.01$	14° 25' 12".9 ± 0".2	"Dominant Center," Moran et al. 1981
H_2O-SOUTH (1)	$19^h\ 21^m\ 26^s.11 \pm 0^s.02$	14° 24' 27".0 ± 0".2	Forster et al. 1978, Moran et al. 1981
H_2O-MAIN	$19^h\ 21^m\ 26^s.21 \pm 0^s.01$	14° 24' 42".9 ± 0".2	
H_2O-SOUTH (2)	$19^h\ 21^m\ 26^s.23 \pm 0^s.02$	14° 24' 35".9 ± 0".3	

REFERENCES

Aitken, D.K., Roche, P.F., and Spenser, P.M. 1981 Preprint.

Becklin, E.E., Telesco, C.M., and Hildebrand, R.H. 1981, in preparation.

Beckwith, S. and Zuckerman, B. 1981, in preparation.

Benson, J.M., and Mutel, R.L., 1980, B.A.A.S. 12, 867.

Bieging, J. 1975, in "H II Regions and Related Topics, eds. T.L. Wilson and D. Downes, (Berlin: Springer-Verlag).

Downes, D., Genzel, R., Moran, J.M., Johnston, K.J., Matveyenko, L.I., Kogan, L.R., Kostenko, V.I., and Rönnäng, B. 1979, Astr. Ap., 79, 233.

Downes, D., Genzel, R., Becklin, E.E. and Wynn-Williams, C.G., 1981, Ap. J., March issue.

Erickson, E.F. and Tokunaga, A.T. 1980, Ap. J. 238, 596

Fomalont, E.B. and Weliachew, L. 1973, Ap. J. 181, 781.

Forster, J.R., Welch, W.J., Wright, M.C.H. and Baundry, A. 1978, Ap. J. 221, 137.

Gatley, I., Becklin, E.E., Werner, M.W., and Harper, D.A. 1978, Ap.J. 220, 822.

Genzel, R. and Downes, D. 1977, Astr. Ap. Suppl. 30, 145.

Genzel, R., Downes, D., Moran, J.M., Johnston, K.J., Spencer, J.H., Matveyenko, L.I., Kogan, L.R., Kostenko, V.I., Rönnäng, B., Haschick, A.D., Reid, M.J., Walker, R.C., Giuffrida, T.S., Burke, B.F. and Moiseev, I.G. 1979, Astr. Ap. 78, 239.

Genzel, R., Downes, D., Schneps, M.H., Reid, M.J., Moran, J.M., Kogan, L.R., Kostenko, V.I., Matveyenko, L.I. and Rönnäng, B. 1981a, Ap. J. submitted.

Genzel, R., Reid, M.J., Moran, J.M. and Downes, D. 1981b, Ap. J. March issue.

Goss, W.M., Knowles, S.H., Balister, M., Batchelor, R.A., and Wellington, K.J., 1976, M.N.R.A.S. 174, 541.

Hackwell, J.A., Grasdalen, G.L. and Gehrz, R.D. 1981, in preparation.

Harper, D.A. 1974, Ap. J. 192, 557.

Harvey, P.M., Hoffmann, W.F. and Campbell, M.F. 1975, Ap. J. Letters 196, L31.

Harwit, M., Soifer, B.T., Houck, J.R., and Pipher, J.L. 1972, Nature Physical Science 236, 103.

Heckman, T.M., and Sullivan, W.T. 1976, Ap. Letters 17, 105.

Högbom, J.A. 1974, Astr. Ap. Suppl. 15, 417.

Mader, G.L., Johnston, K.J. and Moran, J.M. 1978, Ap. J. 224, 115.

Martin, A.H.M. 1972, M.N.R.A.S. 157, 31.

Matsakis, D.N., Bologna, J.M., Schwartz, P.R., Cheung, A.C., Townes, C.H. 1980, Ap.J. 241, 655.

Mezger, P.G., Smith, L.F. and Churchwell, E. 1974, Astr. Ap. 32, 269.

Moran, J.M. et al. 1981, in preparation.

Morris, M. 1976, Ap. J. 210, 100.

Rieke, G.H., Low, F.J. and Kleinmann, D.E. 1972, Ap. J. Letters, 186, L7.

Rodriguez, L.F., Moran, J.M., Ho, P.T.P. and Gottlieb, E.W. 1980, Ap. J. 235, 845.

Rubin, R.H. 1968, Ap. J. 154, 391.

Schneps, M.H., Lane, A.P., Downes, D., Moran, J.M., Genzel, R. and Reid, M.J. 1981, Ap. J. submitted.

Schwab, F. 1980, preprint.

Scott, P.F. 1978, M.N.R.A.S. 183, 435.

Scoville, N.Z. 1980, in IAU Symposium No. 87, Insterstellar Molecules, ed. B. Andrew (Dordrecht: Reidel), in press.

Stein, W.A., and Gillett, F.C. 1969, Ap. J. Letters 155, L197.

Sutton, E., Becklin, E.E., and Neugebauer, G. 1974, Ap. J. Letters 190, L69.

Thronson, H.A. and Harper, D. A. 1979, Ap. J. 230, 133.

Wright, E.L. 1973, Ap. J. 185, 569.

Wynn-Williams, C.G. and Becklin, E.E. 1974, Pub. A.S.P. 86, 5.

Wynn-Williams, C.G., Becklin, E.E. and Neugebauer, G. 1974, Ap. J. 187, 473.

Wynn-Williams, C.G., Becklin, E.E., Matthews, K., Neugebauer, G., and Werner, M.W. 1977, M.N.R.A.S. 179, 255.

Zuckerman, B. 1973, Ap. J. 183, 863.

Zuckerman, B., Kuiper, T.B.H. and Rodriguez-Kuiper, E.N. 1976, Ap. J. Letters 209, L137.

FIGURE CAPTIONS

Figure 1 Infrared and radio continuum emission in W51.

Left: 20 μm map of W51-IRS1 and IRS2 with resolution of 6". The chopper throw was 120" E-W. The contour unit is 1.5 10^{-17} W m^{-2} H_Z^{-1} $ster^{-1}$, or 1.0 Jy per beam area. The dotted rectangle marks the region which contains the strong H_2O maser source W51-MAIN (northern most group of black dots), two weaker H_2O "centers of activity" (middle and southern group of black dots), two OH maser sources and two very compact H II regions (Table 1). The group of dots near the peak of W51-IRS2 marks the H_2O maser source W51-NORTH.

Right: Contours of the 5 GHz free-free continuum emission at a resolution of 2" x 8" (RA x Dec; dashed: Scott 1978) superimposed on the 20 μm map. The radio contours are at 450, 720, 1080, 1440, 2520 and 3600 Kelvins brightness temperature. Note the two ultra-compact H II region in the vicinity of W51-MAIN.

Figure 2 High resolution infrared and radio observations of W51-IRS2.

Bottom: 7.9 μm map of IRS2 at a resolution of 2", relative to the 20 μm peak of IRS2. The contour unit is 5 10^{-17} W m^{-2} Hz^{-1} $ster^{-1}$, or 0.4 Jy per beam area. The chopper throw was 15" North-South. The main peak is IRS2(H_2O), whereas the north-western elongation is IRS2 (H II).

Middle: 20 μm map of IRS2 at a resolution of 2". The contour unit is 1.9 10^{-16} W m^{-2} Hz^{-1} $ster^{-1}$, or 1.4 Jy per beam area. The chopper throw was 15" North-South.

Top: 2 cm radio continuum emission (solid contours) and 6 cm radio continuum emission (dashed), relative to the nominal position of the 20 m peak (bottom and left axes), and in 1950 coordinates (top and right axes). The 2 cm beam was approximately Gaussian with widths (FWHM) 0.4" x 0.7", at a position angle 30° East of North. The 2 cm contour units are 14, 20, 30, 40, 60, 80, 100, 120, 140 and 160 mJy per beam area. The 6 cm beamsize was 1.3" x 2.7", 20° West of North. Only the 20% and 40% contours of the peak are shown, corresponding to 100 and 200 mJy per beam area. The dots are the positions of 22 GHz H_2O maser features (Schneps et al. 1981). The most intense center of H_2O activity is marked "Dominant H_2O Center." The absolute positional uncertainties are ± 0.2" for the radio measurements, and ± 1" for the infrared (shown by a cross for the 20 μm measurements).

Figure 3 Infrared energy distributions taken at the position of the 20 μm peak IRS2(H_2O) and at 4" West, 2.5" North of the 20 μm peak, near the peak of the radio continuum map (IRS2(H II)). The resolution is 2" and the flux density scale was calibrated on β Peg and 4 Lac.

R. GENZEL: Department of Physics, University of California, 557 Birge Hall, Berkeley, CA 94720.

E.E. BECKLIN AND C.G. WYNN-WILLIAMS: Institute for Astronomy, University of Hawaii, 2680 Woodlawn Drive, Honolulu, Hawaii 96822

J.M. MORAN, AND M.J. REID: Harvard-Smithsonian Center for Astrophysics, 60 Garden Street, Cambridge, MA 02138

D.T. JAFFE: Enrico Fermi Institute, University of Chicago, 5630 Ellis Avenue, Chicago IL 60637.

D. DOWNES: Institut de Radio Astronomie Millimetrique, B.P. 391, 38017 Grenoble, FRANCE.

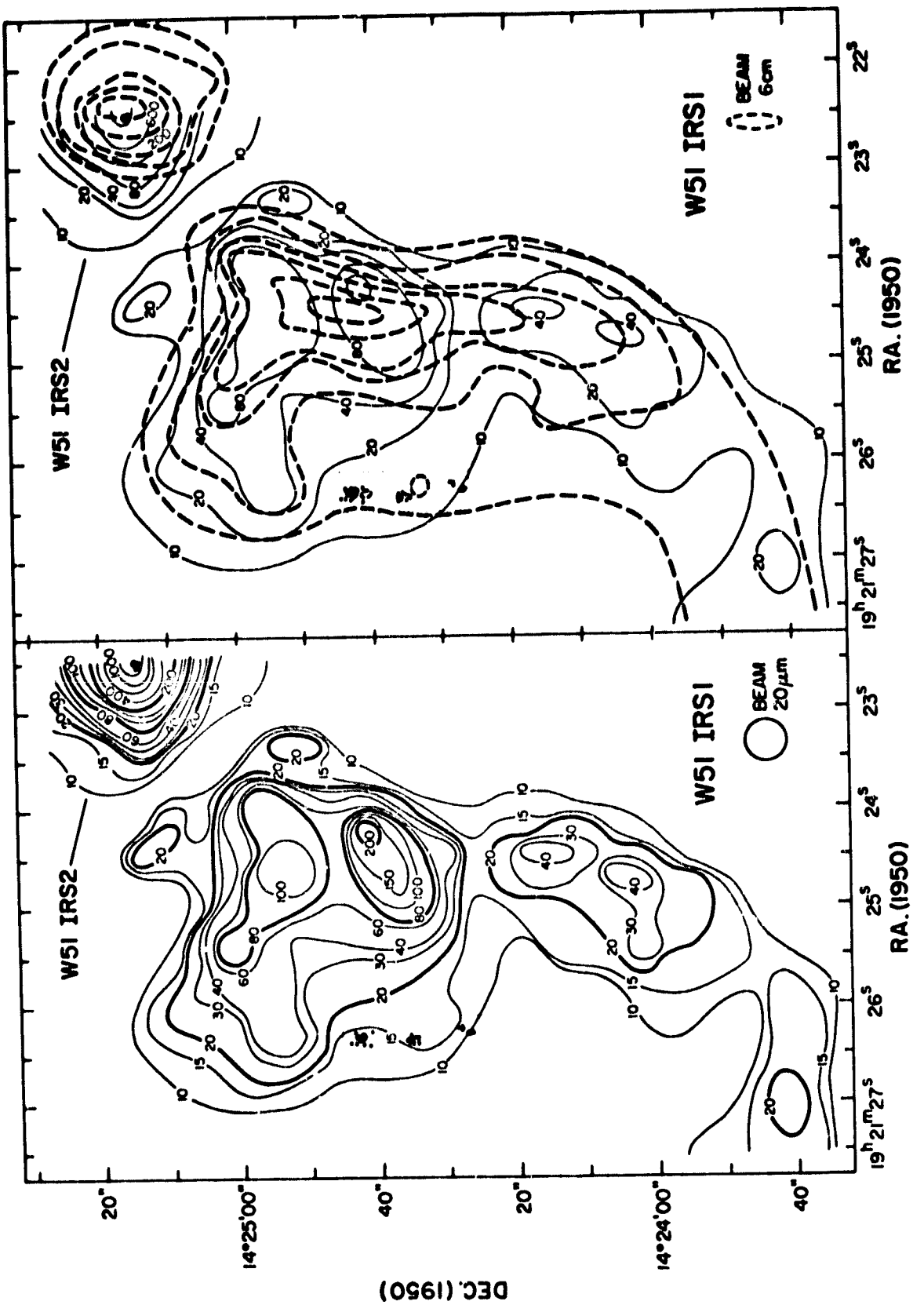
W51 IRS2
W51 IRS1
BEAM 6cm
W51 IRS2
W51 IRS1
BEAM 20μm
RA.(1950)
DEC.(1950)

FIGURE 1

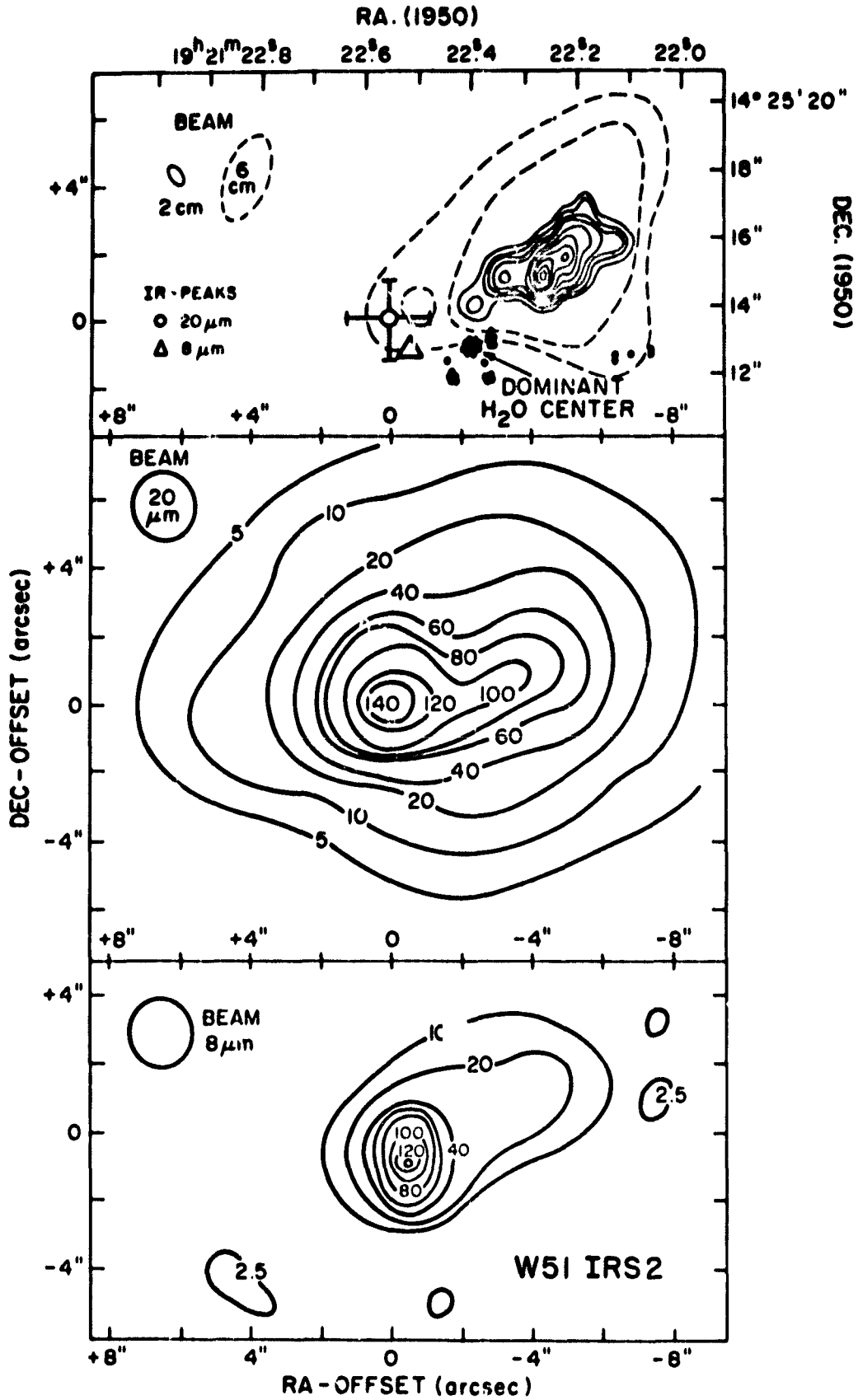
RA. (1950)
19h21m22s.8
22s.6
22s.4
22s.2
22s.0
14° 25' 20"
18"
16"
14"
12"
DEC. (1950)
BEAM
6 cm
2 cm
IR-PEAKS
20 μm
8 μm
DOMINANT
H2O CENTER
+4"
0
+8"
-8"
BEAM
20 μm
5
10
20
40
60
80
100
120
140
DEC-OFFSET (arcsec)
-4"
BEAM
8 μm
2.5
W51 IRS2
4"
RA-OFFSET (arcsec)

FIGURE 2

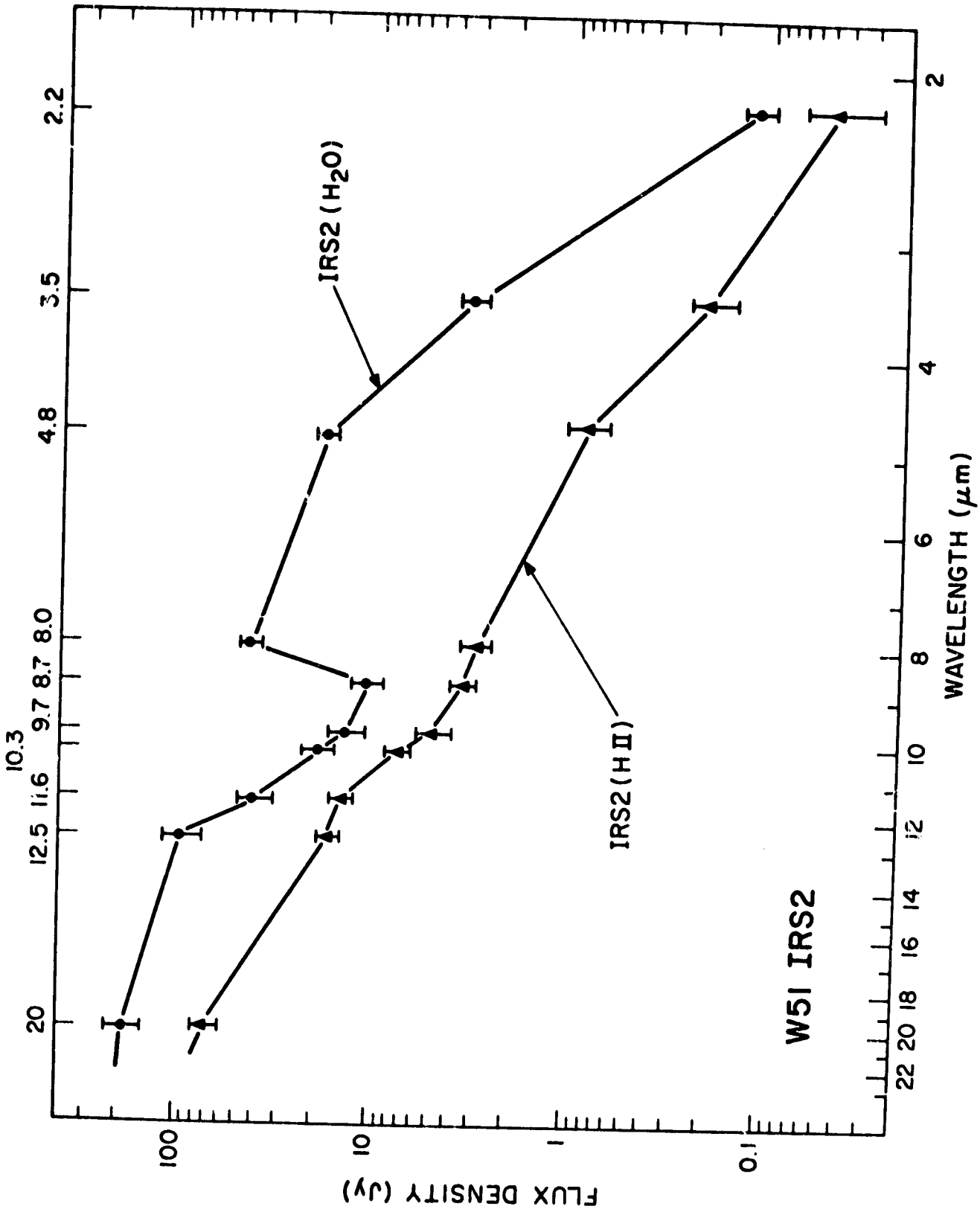
IRS2 (H_2O)
IRS2 (H II)
W51 IRS2
FLUX DENSITY (Jy)
WAVELENGTH (μm)
100
10
1
0.1
20
12.5
11.6
10.3
9.7
8.7
8.0
4.8
3.5
2.2
22
20
18
16
14
12
10
8
6
4
2

FIGURE 3